



ELSEVIER

Contents lists available at ScienceDirect

## Materials and Design

journal homepage: [www.elsevier.com/locate/matdes](http://www.elsevier.com/locate/matdes)

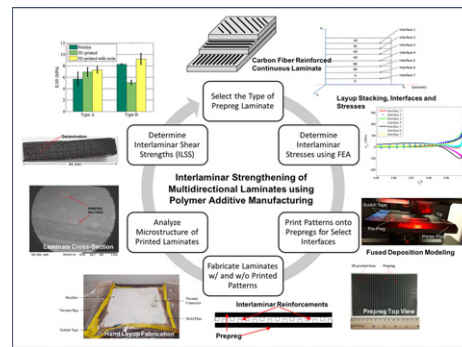
# Interlaminar strengthening of multidirectional laminates using polymer additive manufacturing

M.S. Islam<sup>a</sup>, P. Prabhakar<sup>b,\*</sup><sup>a</sup> Department of Mechanical Engineering, Khulna University of Engineering & Technology, Bangladesh<sup>b</sup> Department of Civil & Environmental Engineering, University of Wisconsin-Madison, WI 53706, United States

## HIGHLIGHTS

- Method to enhance interlaminar properties of multi-directional laminates using polymer additive manufacturing technology.
- Pioneered the printing of patterns onto prepregs at the interlaminar regions for minimizing delamination type failure.
- Interlaminar shear strengths of laminates with different prepreg stacking investigated, which increased by up to 28%.
- Increase in strength attributed to the resistance offered by the printed reinforcements that caused undulated crack path.

## GRAPHICAL ABSTRACT



## ARTICLE INFO

### Article history:

Received 30 January 2017

Received in revised form 24 June 2017

Accepted 20 July 2017

Available online 24 July 2017

### Keywords:

Polymer additive manufacturing

Multi-directional Laminates

Interlaminar Shear Strength

Delamination

Finite element analysis

## ABSTRACT

A novel approach for improving the interlaminar shear strength (ILSS) properties of multi-directional prepreg laminates using polymer additive manufacturing (PAM) technology is proposed in this paper. Fused deposition modeling (FDM) is the PAM technology used for imparting patterns onto carbon prepregs. These modified prepregs are further used for fabricating multi-directional laminates. Prior to manufacturing the laminates, interlaminar regions that are most susceptible to delamination type failure are identified using numerical simulations for selectively reinforcing these critical regions. Next, the influence of printed reinforcements on the ILSS of modified laminates is compared against pristine laminates by conducting short beam shear (SBS) tests. Significant improvement in the ILSS values of up to 28% is observed, which can be attributed to the resistance offered by the printed reinforcements that steered the delamination surfaces along undulated paths as opposed to smooth or straight paths in pristine laminates. Such behavior corroborates the resistance to delamination offered by these printed reinforcements. In summary, this is a pioneering study for exploring the feasibility of using PAM technology for imparting reinforcements at the interlaminar regions in multi-directional laminates with the intention of minimizing delamination.

© 2017 Elsevier Ltd. All rights reserved.

## 1. Introduction

Fiber reinforced polymer matrix composites have a wide range of applications predominantly in the aerospace, automobile and

nuclear industries. In particular, continuous fiber reinforced polymer matrix composites (PMC) are known for their high strength-to-weight and stiffness-to-weight ratios [1]. However, interlaminar matrix regions between the reinforcing fiber layers are critical regions that are highly susceptible to delamination under mechanical loading [2,3]. One of the most common failure mechanisms in layered composites is delamination [4], which may be a result of

\* Corresponding author.

E-mail address: [pprabhakar4@wisc.edu](mailto:pprabhakar4@wisc.edu) (P. Prabhakar).

weak matrix, bad layup, mechanical loading types such as static, impact or fatigue [5–9]. Delamination often introduces internal damage in composites, which could potentially result in the global failure of a component with reduced strength and stiffness.

Earlier researchers have explored different avenues for improving the interlaminar strength of layered composites using techniques like stitching, weaving, z-pinning [10] and braiding [5]. Although, these methods are capable of increasing the through-thickness properties of composites, they have shown to reduce the in-plane properties due to adverse effects like damage in reinforcing fibers or by creating resin rich zones [5,11]. Other methods for enhancing the interlaminar properties include carbon nanotubes (CNTs) dispersed in matrix [12,13] and nanowires synthesized on reinforcing fabric [14–21]. CNTs pose major challenges due to their uneven distribution and tendency towards agglomeration [3,22], and the existing methods for dispersing CNTs in composites tend to damage the fibers [3,12,13] due to high temperature during fabrication. On the other hand, nanowires are synthesized on dry reinforcing fabric, and hence cannot be used with prepreg laminates.

Interlaminar regions in layered composites are typically matrix regions that are weak and render the laminate prone to delamination type failure. In addition, it is widely known that significantly higher interlaminar stresses are manifested at the free edges of multi-directional laminated composites due to property mismatch between different layers. This phenomenon is referred to as “free edge effect” [23,24], which often initiates delamination failure in laminates. Such effects can be minimized by improving the strength and toughness of interlaminar regions that can potentially increase the overall strength of composites. It is proposed here that “the interlaminar strength and toughness of a laminate can be significantly improved by introducing structural reinforcements at the interlaminar regions using polymer additive manufacturing”. Polymer additive manufacturing has the freedom of designing complex patterns easily, which could be extremely useful towards imparting spatially modified smart designs at the interlaminar regions in composites.

In this paper, a novel fabrication technique using polymer additive manufacturing (PAM) is proposed for improving the interlaminar properties of fiber reinforced laminated polymeric composites. It is hypothesized that “the interlaminar shear strength (ILSS) of prepreg laminates can be improved by imparting reinforcing patterns at the interlaminar regions using PAM, also called 3D printing”. Even though it is expected that the fatigue and dynamic behavior of laminates can be improved using this method, only static response in terms of ILSS is considered in this paper as a proof of concept. Towards that, short beam shear (SBS) tests are conducted on unreinforced (called pristine laminates) and reinforced (with 3D printed patterns at the interlaminar regions) laminates for determining their ILSS. A significant improvement in the ILSS values is observed in the reinforced laminates as compared to the unreinforced laminates as will be discussed in detail in later sections.

This paper is organized as follows: Section 2 presents a finite element analysis for determining delamination prone interlaminar regions in multi-directional prepreg laminates. Section 3 provides details of the material system, fabrication and tests conducted. The types of laminates investigated are discussed in Section 3.1, followed by a discussion on materials used for laminates and printed patterns in Section 3.2. The process of printing reinforcements onto carbon prepreps is discussed in Section 3.3 and laminate fabrication in Section 3.4. Details of the short beam shear tests on laminates are provided in Section 3.5. Finally, key results are discussed in Section 4 followed by conclusions.

## 2. Numerically identifying delamination prone interfaces

Multi-directional layered composites manifest significant localized stresses at the interlaminar regions, particularly at free edges

due to mismatch in properties between continuous fiber reinforced layers. This is commonly referred to as the “free edge effect”, which often causes delamination or debonding at the interlaminar regions [24]. Debonding or delamination is observed to be a significant failure mechanism in layered composites with considerable visible damage when subjected to load types like edge-wise/through-thickness compression, flexure, and dynamic impact. Identifying the regions susceptible to high interlaminar stresses will aid in selecting the interlaminar regions that require reinforcements to suppress or reduce the chances of delamination.

Accurate determination of stress distribution near the free edges is very important due to their significant impact on delamination or transverse cracking in laminates. Free edge stress states are three-dimensional in nature [24,25], and classical lamination theory (CLT) is unable to determine these stresses accurately. Therefore, various analytical and numerical approaches such as finite difference, finite element, closed form analytical approach, boundary layer theories and layer-wise theories have been developed by earlier researchers to calculate interlaminar stresses. Martin et al. [26] presented a variational framework of Pipes and Pagano's [27] generalized plane strain formulation for free edge effect, which was used in this paper to determine interlaminar stresses. Stress distribution at the interfaces were determined by implementing this generalized plane strain formulation (called Quasi-2D) within the finite element framework in ABAQUS, a commercially available software. Detailed derivation and implementation of the Quasi-2D modeling approach for capturing free edge effects in laminates under thermo-mechanical loading is presented in a published article by the current authors in Islam and Prabhakar [28].

A sixteen layer multi-directional laminate with a stacking sequence of  $[+45_2/-45_2/90_2/0_2]_s$  was modeled, and the schematic of its cross-section is shown in Fig. 1 (a). All the layers were assumed to be of equal thickness. Stacking sequence represents the in-plane orientation of continuous fibers in each layer (see Fig. 1 (b)), where the layers are stacked in the through-thickness direction. In the stacking sequence mentioned above, there are two layers oriented at  $45^\circ$  about the X-axis, two layers oriented at  $-45^\circ$  two layers oriented at  $90^\circ$  and two layers oriented along the X-axis. Due to symmetry of stacking sequence in the through-thickness direction, only 8 layers with symmetry boundary condition at the mid-plane of the laminate were modeled.

Each layer of the laminate was assumed to be elastic transversely isotropic homogenized material for modeling purposes. Typical properties of continuous carbon fiber reinforced lamina were obtained from Prabhakar and Waas [29]. Interfaces between any two layers were treated as perfectly bonded, and stress distribution along each of these interfaces was determined. The goal of computing the interlaminar stresses in unmodified perfectly bonded multi-directional laminates was to identify critical interlaminar regions with higher stresses, which served as a guide for identifying regions prone to damage. The numerical analysis of laminates with interlaminar reinforcements involves further in-depth computational framework, which is outside the scope of this paper.

Interlaminar stresses caused due to axial loading were determined. Fig. 2 (a) and Fig. 2 (b) shows the interlaminar normal stress ( $\sigma_{33}$ ) and shear stress ( $\sigma_{23}$ ) distributions in the eight layer model. It is observed from Fig. 2 that the free edge interlaminar stresses are higher at interfaces 2, 4 and 6 as compared to other interfaces. This implies that the interfaces between layers of dissimilar fiber orientations ( $+45/-45, -45/90$ , etc.) experience higher stress than similar interfaces ( $+45/+45, 90/90$ , etc.). For the stacking sequence chosen, these dissimilar interfaces were modified using polymer additive manufacturing with an expectation of increasing the overall interlaminar shear strength of the laminate, as will be discussed in the following section.

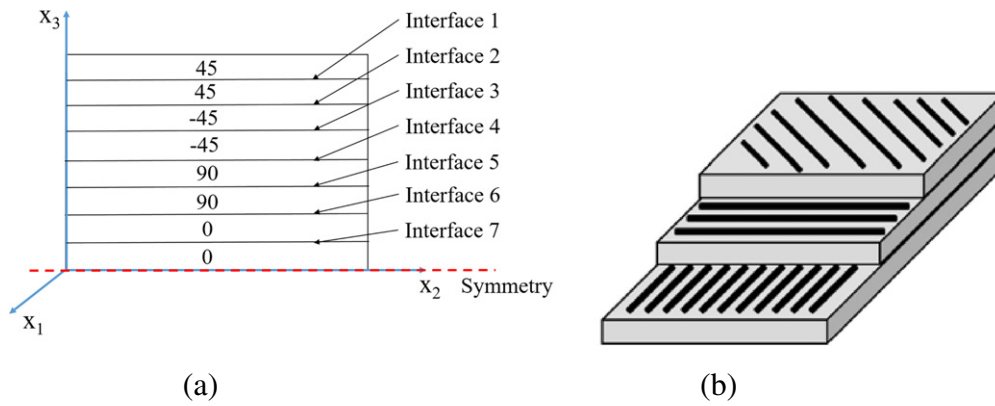


Fig. 1. (a) Schematic of cross-section of a laminate; (b) Stacking of continuous fiber reinforced layers in a multi-directional laminate.

### 3. Experimental details

#### 3.1. Types of laminates investigated

Two laminates, namely Type A and Type B, with 40 layers each were investigated in this paper. Stacking sequence of  $[+45_5 / -45_5 / 90_5 / 0 - 5]_s$  and  $[+45_3 / -45_3 / 90_3 / 0_3 / +45_2 / -45_2 / 90_2 / 0_2]_s$  were chosen for Type A and Type B laminates, respectively. Both these types of laminates were manufactured under three conditions: pristine, printed interfaces and printed interfaces with additional resin. In the pristine condition, laminates were manufactured using prepreg layers without additional surface modifications. These pristine laminates serve as the baseline. In the laminates with printed interfaces, interlaminar regions identified numerically as prone to delamination were modified using PAM (refer to Section 3.3). As will be discussed later in Section 4, voids were observed at the interlaminar regions due to the introduction of printed patterns on prepreg layers. Additional resin was used to eliminate/reduce these voids, and this condition was referred to as “printed interfaces with additional resin”.

#### 3.2. Material system

Unidirectional carbon fiber prepreg tapes purchased from CST Composites ([www.cstsales.com](http://www.cstsales.com)) were used to fabricate the multi-directional laminates. Material properties of carbon fiber prepreps are given in Table 1. Epon 862 with EPIKURE 9553 hardener was used as additional resin in samples with printed interlaminar patterns to

reduce voids in the laminate. The hardener was mixed with the resin at a weight ratio of 16.9:100, as recommended by the manufacturer.

#### 3.3. Printing on prepreps

Interlaminar reinforcements were introduced on prepreg layers using fused deposition modeling (FDM) technique. These prepreps were then used to fabricate the laminates. MakerBot Replicator desktop 3D printer (Fig. 3 (a)) was used to print patterns on prepreps. Typically, the printing process starts on a printer plate in the form of raft or support upon which the actual part is printed. In the current case, the challenge was to print patterns directly onto a prepreg without printing any raft or support. Towards that, the prepreps were attached onto the printer plate with scotch tape as shown in Fig. 3 (b).

Poly(lactic acid) (PLA) was used as the printing material with nozzle printing temperature of 215 °C. It should be noted here that PLA is a biodegradable and bioactive thermoplastic material and may pose issues regarding compatibility with epoxy matrix. However, the aim of this study was to explore the feasibility of imparting structural patterns at the interlaminar regions. Having said that, it is critical to investigate the influence of other compatible materials as potential reinforcements. Fig. 4 (a) displays the top view of a prepreg with printed lines and Fig. 4 (b) shows the schematic of the cross-section with print dimensions. The printed lines were 0.65 mm wide and 0.25 mm thick with 2.6 mm spacing between two successive lines as shown in Fig. 4 (b).

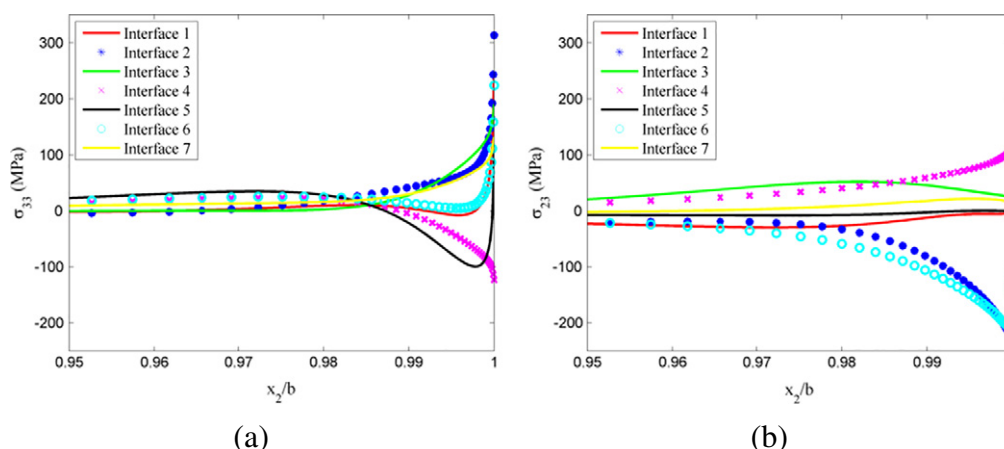


Fig. 2. Distribution of interlaminar stresses along different interfaces of  $[45_2 / -45_2 / 90_2 / 0_2]_s$  laminate: (a) normal stress  $\sigma_{33}$  and (b) shear stress  $\sigma_{23}$

**Table 1**  
Prepregs properties (<http://www.cstsales.com>).

Properties	prepregs
Fiber aerial weight	150 gm/m <sup>2</sup>
Resin content	35 %
Thickness	0.005–0.006 in.

### 3.4. Laminate fabrication

Hand layup composite fabrication method was used to manufacture the multi-directional laminates using prepreg layups. The fabrication procedure is briefly outlined here. A release agent was first applied on one surface each of two aluminum mold plates. Prepreg layers were then placed between the two aluminum mold plates with a chosen stacking sequence, followed by enclosing the setup in a bagging film. The bag was sealed and drawn to vacuum using a vacuum pump. The entire enclosed setup was next placed inside an oven for curing following a prescribed temperature profile. As suggested by the manufacturers, the layup was cured at 135 °C for 1 h and the laminate was removed from the bag after 24 h.

In the case of laminates with printed interfaces and additional resin, a brush was used to apply the extra amount of resin on the

printed surface of a prepreg prior to stacking the next layup on top. The prepreg layups were arranged such that the printed lines form a teeth-like structure at the interfaces of dissimilarly oriented layups. Schematic of an interlaminar region (interfaces) with printed reinforcing patterns is shown in Fig. 5. It was hypothesized that such a pattern would provide shear resistance to the formation of new surfaces, thereby, suppressing the ease of delamination.

### 3.5. Short beam shear test

Short beam shear (SBS) tests were conducted to measure the interlaminar shear strength (ILSS) values of the fabricated laminates. Five specimens for each type of laminate and fabrication condition were tested according to the ASTM D2344 standard. Dimensions of the test specimens were maintained such that the span length = thickness x 4 and width = thickness x 2. SBS tests were conducted on Instron 8801 machine at a loading rate of 1.0 mm/min. Load-displacement responses were determined from the SBS tests, and their interlaminar shear strength values were calculated using:

$$F_{sbs} = 0.75 \times \frac{P_m}{b \times h} \tag{1}$$



**Fig. 3.** (a) MakerBot Replicator desktop 3D printer and (b) 3D printing on prepregs.

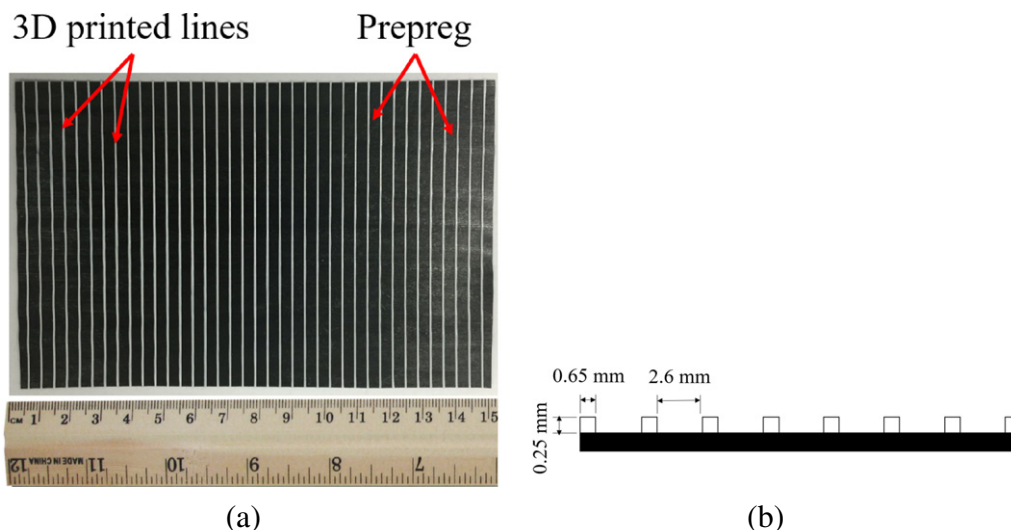


**Fig. 4.** (a) 3D printed lines on prepreg; (b) Schematic of cross-section of 3D printed prepreg.

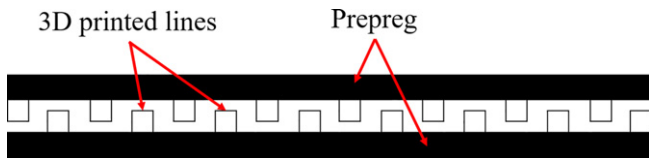


Fig. 5. Formation of 3D printed interlaminar reinforcement.

where,  $F_{sbs}$  = short-beam strength (MPa),  $P_m$  = maximum load observed during the test (N),  $b$  = measured specimen width (mm) and  $h$  = measured specimen thickness (mm).

#### 4. Results and discussions

Multi-directional prepreg laminates with and without modified interlaminar regions were investigated in this paper in order to determine the influence of interlaminar modifications on their ILSS. It should be noted that tensile properties are fiber dominated and ILSS is a matrix dominated property [30], which makes ILSS a good measure of the influence of modifications at the interlaminar matrix rich regions. Prior to discussing the experimental results from the SBS tests, key observations from the microscopic analyses of the laminate cross-sections are discussed first.

##### 4.1. Analysis of microstructure

Fig. 6 shows the cross-sections of Type A and B laminates with patterns printed at the interlaminar regions. Elliptical regions in these images represent the cross-section of the printed lines. Type B (Fig. 6 (b)) laminate appears to manifest more voids (black regions) as compared to Type A (Fig. 6 (a)) laminate. As described above, Type B laminate has higher number of interfaces with printed reinforcements as compared to Type A laminate. The amount of resin in prepreps is insufficient to wet the large number of printed patterns in Type B laminate, which results in more voids.

Type A laminate has 6 interfaces with printed patterns, and the prepreg resin is almost sufficient to wet the printed lines as observed in Fig. 6 (a). However, Type B laminate consists of 14 interfaces with printed patterns, and the prepreg resin is insufficient to cover all the printed lines causing more voids in the laminate as shown in Fig. 6 (b). As a remedial solution to void formation, additional resin was applied on the printed surfaces of prepreps during fabrication as was mentioned earlier in Section 3.1. Fig. 7 shows the cross-section of Type A and B laminates with additional resin, which exhibit very few voids as compared to the previous case (Fig. 6).

##### 4.2. Interlaminar shear strength

ILSS values of Type A and B laminates fabricated under the three different conditions (pristine, 3D printed interface and 3D printed interface with additional resin) are shown in Fig. 8. ILSS values appear to increase by an average of 21.30% for Type A laminates with printed pattern as compared to pristine Type A laminates, and approximately 28.35% improvement with additional resin added. This increase in ILSS can be attributed to the shear resistance offered by the PAM reinforcements constructed along the critical interfaces. It should be noted here that the improvement in ILSS with additional resin added is small as compared to the ones without. This is because the voids present in Type A laminates due to printed patterns is insignificant as shown in Fig. 6 (a).

In contrast, the ILSS values decreased by about 38.86% for Type B laminates with printed interfaces as compared to the pristine ones. This is primarily attributed to the voids formed during laminate fabrication due to insufficient resin in the prepreg (refer to Fig. 6 (b)). These voids act as a damage initiating catalyzers, which effectively reduce the ILSS values. However, an increase in ILSS values by approximately 11.26% with additional resin was observed in Type B laminates. All these results are summarized in Table 2 along with the percentage increase in laminate thickness corresponding to different interface modifications. The overall laminate thickness depends on the size of print lines, which is a limitation of the printer nozzle. Finer print lines are expected to reduce the overall thickness of the laminate, while improving the ILSS further.

Previous researchers have determined the ILSS values for fiber reinforced laminates with various interlaminar reinforcements. Fan et. al. [12] examined the influence of multi-walled carbon nanotube (MWCNT) reinforcement on glass fiber reinforced epoxy composites and established a maximum increase in ILSS values by  $\approx 33\%$ . Zhu et. al. [31] investigated the effect of carbon nanotube enhancement of glass fiber reinforced vinyl ester composite and established an improvement of ILSS by a maximum of 45%. Du et. al. [32] observed that the ILSS increased by 14 to 25% in stitched GFRP prepreg tape composites. In the current paper, a 28.35% increase in the ILSS values of prepreg laminates by PAM interlaminar reinforcements was observed, which is similar to the improvement obtained from other methods [12,31,32]. The added advantage of the PAM technique is the design freedom and precision with which the spatial distribution of interlaminar patterns can be achieved.

Figs. 9 and 10 show the through-thickness images of Type A and B failed specimens, respectively. The key failure mechanism in both types of laminates was delamination along the interlaminar regions. Here, Fig. 9 (b) and Fig. 10 (b) show a typical failed sample of Type A

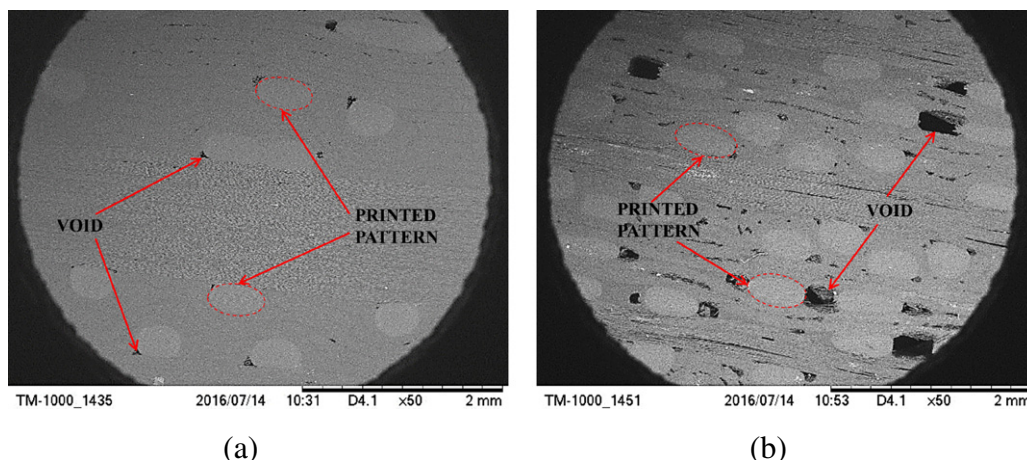


Fig. 6. Cross-section of (a) Type A and (b) Type B laminates with 3D printed interlaminar regions.

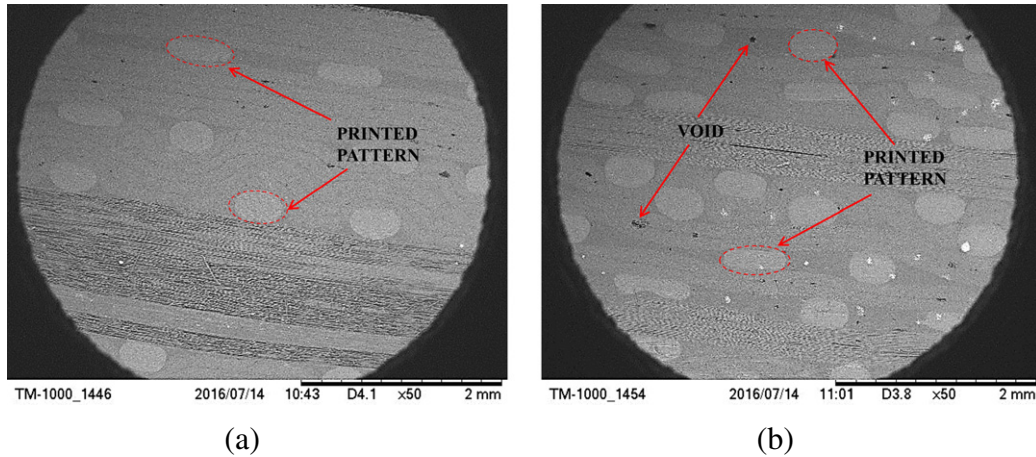


Fig. 7. Cross-section of (a) Type A and (b) Type B laminates with 3D printed interlaminar regions with additional resin.

and B laminates with printed interfaces and additional resin added. In both Type A (Fig. 9 (a)) and B (Fig. 10 (a)) laminates with no interlaminar reinforcement, delamination lines appear smooth and straight with no undulations along the length of the specimen. However, the delamination lines appear undulated in laminates with printed interfaces. This implies that the area of new surfaces formed was higher than that in the pristine case, which is an important contributor to the improved ILSS values.

In this paper, the printed patterns at the interfaces were straight lines along the width of samples that were evenly spaced along their length. However, one of the main objectives of using 3D printing is the ability to vary these patterns spatially to suppress the susceptibility of interlaminar regions from delamination that initiate at the free edges. Therefore, there is a huge potential of expanding the work presented here towards this particular application, which has not been reported here. The main objective of this paper was to establish the feasibility of using PAM towards improving ILSS for multi-directional laminates.

5. Conclusions

In this paper, a novel method to enhance the interlaminar properties of multi-directional laminates using polymer additive manufacturing technology was proposed. The primary goal of the research presented in this paper was to explore the influence of modifying the

interlaminar regions on the interlaminar shear strength (ILSS) values of continuous carbon fiber reinforced prepreg laminates. Patterns of reinforcements were printed onto the carbon prepregs using fused deposition modeling technique for imparting interlaminar modifications. Two types of laminates were fabricated, namely Type A and B, where the prepreg stacking were chosen such that the number of interlaminar regions to be reinforced changed between the two types. Within each type of laminate, three different conditions prevailed - pristine, printed interfaces, and printed interfaces with additional resin. Key observations and conclusions of this paper are summarized as follows:

1. The ILSS values of laminates with modified interlaminar regions manifested an increase of approximately 28% and 11% for Type A and Type B laminates, respectively. This was achieved by introducing additional resin at the interlaminar regions with printed reinforcements.
2. It was observed that as the number of modified interlaminar regions (printed interfaces) increased, the pre-existing resin in the prepreg was insufficient for wetting the printed reinforcements. This resulted in undesired voids in the laminate. Therefore, additional resin may be required in the case of modifying several interlaminar regions in a laminate.
3. The increase in ILSS with modified interlaminar regions can be attributed to the resistance offered by the printed reinforcements. That is, the new surfaces created due to delamination during short beam shear tests were undulated in the modified laminates as opposed to smooth or straight regions in pristine samples. Such behavior corroborates the resistance to delimitation offered by these printed reinforcements.
4. Finally, it should be noted that printed reinforcements may increase the overall thickness of a laminate, which can be

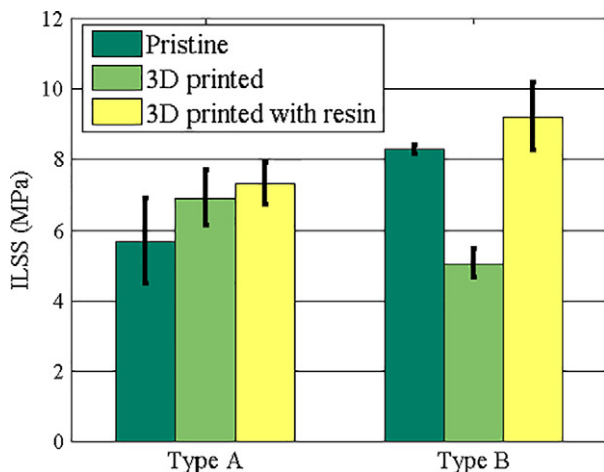


Fig. 8. Interlaminar shear strength values.

Table 2 Comparison of ILSS of different laminates.

Type	Thickness (mm)	% Increase	ILSS (MPa)	% Increase
A pristine	5.31	–	5.68 ± 1.2	–
A 3D printed	6.39	20.34	6.89 ± 0.78	21.30
A 3D printed with resin	6.66	25.42	7.29 ± 0.58	28.35
B pristine	5.44	–	8.26 ± 0.12	–
B 3D printed	7.03	29.94	5.05 ± 0.41	–38.86
B 3D printed with resin	7.92	46.70	9.19 ± 0.96	11.26

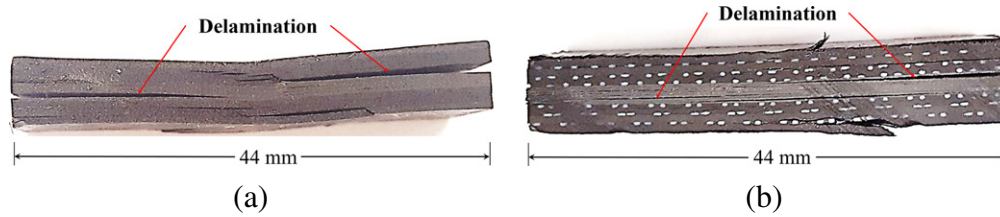


Fig. 9. Failed sample of Type A laminate: (a) pristine and (b) 3D printed interface with additional resin.

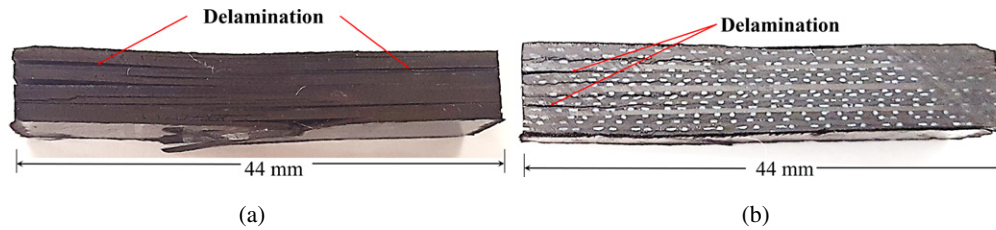


Fig. 10. Failed sample of Type B laminate: (a) pristine and (b) 3D printed interface with additional resin.

minimized by printing fine patterns at the interlaminar regions by choosing 3D printers with finer print nozzles.

In conclusion, this is a pioneering study for exploring the feasibility of using polymer additive manufacturing technology for imparting reinforcements at the interlaminar regions in multi-directional laminates with the intention of minimizing delamination type failure. Nonetheless, this paper has only scratched the surface of the enormous potential of using this technology for interlaminar reinforcements in laminates, especially, in view of free edge effects, fatigue and dynamic loading.

#### Acknowledgments

The authors would like to acknowledge the support through the AFOSR Young Investigator Program (grant no.: FA9550-15-1-0216) for conducting the research presented here.

#### References

- [1] M.M. Pavlick, W.S. Johnson, B. Jensen, E. Weiser, Evaluation of mechanical properties of advanced polymers for composite cryotank applications, *Compos. Part A: Appl. Sci. Manuf.* 40 (4) (2009) 359–367.
- [2] U. Galan, Y. Lin, G.J. Ehlert, H.A. Sodano, Effect of ZnO nanowire morphology on the interfacial strength of nanowire coated carbon fibers, *Compos. Sci. Technol.* 71 (7) (2011) 946–954.
- [3] S.S. Wicks, W. Wang, M.R. Williams, B.L. Wardle, Multi-scale interlaminar fracture mechanisms in woven composite laminates reinforced with aligned carbon nanotubes, *Compos. Sci. Technol.* 100 (2014) 128–135.
- [4] A. Szekrenyes, Overview on the experimental investigations of the fracture toughness in composite materials, *Hungarian Electronic Journal of Sciences*, <http://hej.sze.hu/>, Mechanical Engineering Section, MET-020507-A, 2002.
- [5] K.A. Dransfield, L.K. Jain, Y. Mai, On the effects of stitching in CFRPS. Mode I delamination toughness, *Compos. Sci. Technol.* 58 (6) (1998) 815–827.
- [6] A. Argüelles, J. Viña, A.F. Canteli, M.A. Castrillo, J. Bonhomme, Interlaminar crack initiation and growth rate in a carbon-fibre epoxy composite under mode-I fatigue loading, *Compos. Sci. Technol.* 68 (12) (2008) 2325–2331.
- [7] R. Khan, C.D. Rans, R. Benedictus, Effect of stress ratio on delamination growth behavior in unidirectional carbon/epoxy under mode I fatigue loading, *Proc. ICCM. Edinburgh* (2009).
- [8] R. Rikards, F.G. Buchholz, A.K. Bledzki, G. Wacker, A. Korjakin, Mode I, mode II, and mixed-mode I/II interlaminar fracture toughness of GFRP influenced by fiber surface treatment, *Mech. Compos. Mater.* 32 (5) (1996) 439–462.
- [9] T.K. O'Brien, *Characterization of delamination onset and growth in a composite laminate, Damage in Composite Materials: Basic Mechanisms, Accumulation, Tolerance, and Characterization*, ASTM International, 1982.
- [10] P. Robinson, S. Das, Mode I DCB testing of composite laminates reinforced with z-direction pins: a simple model for the investigation of data reduction strategies, *Eng. Fract. Mech.* 71 (3) (2004) 345–364.
- [11] R.J. Sager, P.J. Klein, D.C. Davis, D.C. Lagoudas, G.L. Warren, H. Sue, Interlaminar fracture toughness of woven fabric composite laminates with carbon nanotube/epoxy interleaf films, *J. Appl. Polym. Sci.* 121 (4) (2011) 2394–2405.
- [12] Z. Fan, M.H. Santare, S.G. Advani, Interlaminar shear strength of glass fiber reinforced epoxy composites enhanced with multi-walled carbon nanotubes, *Compos. Part A: Appl. Sci. Manuf.* 39 (3) (2008) 540–554.
- [13] B. Ashrafi, J. Guan, V. Mirjalili, Y. Zhang, L. Chun, P. Hubert, B. Simard, C.T. Kingston, O. Bourne, A. Johnston, Enhancement of mechanical performance of epoxy/carbon fiber laminate composites using single-walled carbon nanotubes, *Compos. Sci. Technol.* 71 (13) (2011) 1569–1578.
- [14] A.G. Castellanos, M.S. Islam, M.A.I. Shuvo, Y. Lin, P. Prabhakar, Nanowire reinforcement of woven composites for enhancing interlaminar fracture toughness, *J. Sandw. Struct. Mater.* (2016)1099636216650989.
- [15] A. Castellanos, M.S. Islam, S. Quevedo, M.A.I. Shuvo, Y. Lin, P. Prabhakar, Nanowire stiffening of woven composites towards enhancing interlaminar fracture toughness, *American Society of Composites-30th Technical Conference*, 2015.
- [16] A. Castellanos, M.S. Islam, M.A.I. Shuvo, Y. Lin, P. Prabhakar, Impact response of woven composites with interlaminar reinforcement, *57th AIAA/ASCE/AHS/ASC Structures, Structural Dynamics, and Materials Conference*, 2016, pp. 1236.
- [17] K. Kong, B.K. Deka, S.K. Kwak, A. Oh, H. Kim, Y. Park, H.W. Park, Processing and mechanical characterization of ZnO/polyester woven carbon-fiber composites with different ZnO concentrations, *Compos. Part A Appl. Sci. Manuf.* 55 (2013) 152–160.
- [18] H. Hwang, M.H. Malakooti, B.A. Patterson, H.A. Sodano, Increased interlayer friction through ZnO nanowire arrays grown on aramid fabric, *Compos. Sci. Technol.* 107 (2015) 75–81.
- [19] J.B. Baxter, E.S. Aydil, Nanowire-based dye-sensitized solar cells, *Appl. Phys. Lett.* 86 (5) (2005) 053114.
- [20] X. Wang, J. Song, J. Liu, Z.L. Wang, Direct-current nanogenerator driven by ultrasonic waves, *Science* 316 (5821) (2007) 102–105.
- [21] Y. Lin, G. Ehlert, H.A. Sodano, Increased interface strength in carbon fiber composites through a ZnO nanowire interphase, *Adv. Funct. Mater.* 19 (16) (2009) 2654–2660.
- [22] K. Kong, B.K. Deka, M. Kim, A. Oh, H.W. Kim, Y. Park, H. Park, Interlaminar resistive heating behavior of woven carbon fiber composite laminates modified with ZnO nanorods, *Compos. Sci. Technol.* 100 (2014) 83–91.
- [23] R.B. Pipes, I.M. Daniel, Moire analysis of the interlaminar shear edge effect in laminated composites, *J. Compos. Mater.* 5 (2) (1971) 255–259.
- [24] D. Zhang, J. Ye, H.Y. Sheng, Free-edge and ply cracking effect in cross-ply laminated composites under uniform extension and thermal loading, *Compos. Struct.* 76 (4) (2006) 314–325.
- [25] M. Tahani, A. Nosier, Free edge stress analysis of general cross-ply composite laminates under extension and thermal loading, *Compos. Struct.* 60 (1) (2003) 91–103.
- [26] E. Martin, D. Leguillon, N. Carrère, A twofold strength and toughness criterion for the onset of free-edge shear delamination in angle-ply laminates, *Int. J. Solids Struct.* 47 (9) (2010) 1297–1305.
- [27] R.B. Pipes, N.J. Pagano, Interlaminar stresses in composite laminates under uniform axial extension, *J. Compos. Mater.* 4 (4) (1970) 538–548.
- [28] M.S. Islam, P. Prabhakar, Modeling framework for free edge effects in laminates under thermo-mechanical loading, *Compos. Part B: Eng.* 116 (2017) 89–98.

- [29] P. Prabhakar, A.M. Waas, Upscaling from a micro-mechanics model to capture laminate compressive strength due to kink banding instability, *Comput. Mater. Sci.* 67 (2013) 40–47.
- [30] M.S. Islam, E. Melendez-Soto, A.G. Castellanos, P. Prabhakar, Investigation of woven composites as potential cryogenic tank materials, *Cryogenics* 72 (2015) 82–89.
- [31] J. Zhu, A. Imam, R. Crane, K. Lozano, V.N. Khabashesku, E.V. Barrera, Processing a glass fiber reinforced vinyl ester composite with nanotube enhancement of interlaminar shear strength, *Compos. Sci. Technol.* 67 (7) (2007) 1509–1517.
- [32] X. Du, F. Xue, Z. Gu, Experimental study of the effect of stitching on strength of a composite laminate, *Proceedings of the international symposium on composite materials & structures*, 1986, pp. 10–13.